Chinese Journal of Electronics
vol. 33, no. 1, pp. 153–160, January 2024
https://doi.org/10.23919/cje.2022.00.272

RESEARCH ARTICLE

Graph Signal Reconstruction from Low-Resolution Multi-Bit Observations

Zhaoting LIU, Chen YU, Yafeng WANG, and Shuchen LIU

School of Communication Engineering, Hangzhou Dianzi University, Hangzhou 310018, China

Corresponding author: Zhaoting LIU, Email: liuzht@hdu.edu.cn
Manuscript Received August 12, 2022; Accepted November 22, 2022

Abstract — Low hardware cost and power consumption in information transmission, processing and storage is an urgent demand for many big data problems, in which the high-dimensional data often be modelled as graph signals. This paper considers the problem of recovering a smooth graph signal by using its low-resolution multi-bit quantized observations. The underlying problem is formulated as a regularized maximum-likelihood optimization and is solved via an expectation maximization scheme. With this scheme, the multi-bit graph signal recovery (MB-GSR) is efficiently implemented by using the quantized observations collected from random subsets of graph nodes. The simulation results show that increasing the sampling resolution to 2 or 3 bits per sample leads to a considerable performance improvement, while the energy consumption and implementation costs remain much lower compared to the implementation of high resolution sampling.
Keywords — Graph signal reconstruction, Maximum-likelihood, Expectation maximization, Low-bit quantization.
Citation — Zhaoting LIU, Chen YU, Yafeng WANG, *et al.*, "Graph Signal Reconstruction from Low-Resolution Multi-Bit Observations," *Chinese Journal of Electronics*, vol. 33, no. 1, pp. 153–160, 2024. doi: 10.23919/cje.2022.00.272.

I. Introduction

Modern information processing frequently involves a large volume of increasingly complex data generated from various data sources. The complexity comes, in particular, from the intrinsic relationship and structure of the framework on which these data resides. For instance, environmental monitoring data obtained at different regions are related to their geographical proximities, traffic volumes at different locations in a transportation network depends on the topology of the network, and individual preferences of a group of persons may be influenced by the friendships among them. As powerful mathematical tools, graphs offer the ability to efficiently model relationships and structures of such complex data (denoted as graph signals). This makes signal processing on graphs, or graph signal processing (GSP) [1]–[3], become an emerging research field, and it has attracted growing interests recently in the signal processing community.

One of the basic problems in GSP is the development of graph signal reconstruction [4]–[7] from inaccurate and incomplete data. Typically, the graph signals are bandlimited [8] or the graph signal is smooth [9] with respect to the graph topology, i.e., the signal changes between neighboring nodes are small. By exploiting this spatial relationship of graph signal, the unknown data associated with unsampled nodes can be reconstructed from the sampled data. Over the past few years, there has been much work devoted to the graph signal reconstruction from sampled, noisy, missing, or corrupted measurements. The most approaches, with samples collected from random subsets of graph nodes, solve least-squares problems penalized with different regularizers. They recovers the smooth graph signal in both the time-static and time-varying cases [10], [11] by balancing a trade-off between data-fitting and smoothness quantified in terms of Tikhonov regularization (i.e, graph Laplacian quadratic form) or total variation regularization. To recover a bandlimited (or approximately bandlimited) graph signal from a subset of its samples, graph sampling strategies [12]–[15] have been studied to optimize the selection of the sampling set. In addition, the graph signal reconstruction in a distributed manner [11], [12] also has

Associate Editor: Prof. Lin WANG, Xiamen University.

received attention in order to process the large-scale graph-structured data in lack of a central processor.

Most of the graph signal recovery algorithms are based on the assumption that quantization errors are negligible as a result of using high-resolution analog-to-digital converters (ADCs). However, using high resolution ADCs is usually expensive and power-hungry [16]–[19]. In this paper, as opposed to the previous works, we aim to investigate the problem of recovering smooth graph signals from low-resolution few-bit measurements, which are taken over only a partial set of nodes. In such cases, contrary to the high-resolution or full precise quantization case, the available measurements containing large quantization errors can not be directly employed for the graph signal recovery. Although there are many well-known techniques for the classical signal reconstruction by using the low-bit techniques, they can not be directly applied to the graph signal reconstruction. One reason is that graph signals are smooth, in other words, they vary slowly across the nodes. This feature makes it difficult to quantify graph signals without prior knowledge of their distribution. To solve this problem, we consider to use a random dithering scheme which makes the graph signal samples vary randomly across the nodes and no longer smooth. This naturally raises a question, whether the underlying smoothness can still be used to reconstruct the graph signals of the entire network from the graph signal quantized samples of a small number of nodes? Our study will prove that this answer is yes. We develop regularized maximum-likelihood optimization algorithms for graph signal recovery. The proposed algorithm employs an iterative scheme based on expectation maximization to retrieve the raw unquantized observations and recover the graph signals from low-bit quantized observations. The simulation results show that the graph signal recovery performance can be greatly improved when increasing the sampling resolution from 1 bit to 2 or 3 bits, while the power consumption and implementation costs remain much lower than the high-resolution sampling scenario.

II. Graph Signal Model and Problem Formulation

1. Graph signal model

We consider signals on an undirected, connected and weighted graph $\mathcal{G}=(\mathcal{V},\mathcal{E},\boldsymbol{W})$ with node set $\mathcal{V}\triangleq\{1,2,\ldots,K\}$, edge set $\mathcal{E}\subseteq\mathcal{V}\times\mathcal{V}$, and weight matrix $\boldsymbol{W}\in\mathbb{R}^{K\times K}$. The entries $w_{ij}=w_{ji}\geq 0$ of the weight matrix are non-zero if and only if $(i,j)\in\mathcal{E}$. The weights w_{ij} describe the strength of the connection from node i to j. We assume $w_{ii}=0$ for all $i\in\mathcal{V}$, that is, the graph has no loops.

A graph signal is a mapping from the node set $\mathcal{V}$ to $\mathbb{R}$, i.e., it associates with each node $i\in\mathcal{V}$ a real number $x_i\in\mathbb{R}$. These real numbers can be conveniently arranged into a length-K vector $\boldsymbol{x}\triangleq[x_1,x_2,\ldots,x_K]^{\mathsf{T}}\in\mathbb{R}^K$. It has been shown that, if $\boldsymbol{x}$ is smooth in the sense that it varies little over strongly connected nodes, it is possible to recover the graph signal $\boldsymbol{x}$ from its $M<K$ noisy samples: $\boldsymbol{y}^s[n]=\big[y_{k_{1n}}[n],y_{k_{2n}}[n],\ldots,y_{k_{Mn}}[n]\big]^{\mathsf{T}}\in\mathbb{R}^M$ taken over a random subset of nodes,

$$\mathcal{V}^s[n]\triangleq\{k_{1n},k_{2n},\ldots,k_{Mn}\}\subseteq\mathcal{V} \tag{1}$$

at time n. Note that, in the fixed sampling case, the subset $\mathcal{V}^s[n]$ is constant, i.e., $\mathcal{V}^s[n]=\mathcal{V}^s$ for any n. Our work in this paper covers this special case. With (1), the noisy samples $\boldsymbol{y}^s[n]$ is related to $\boldsymbol{x}$ via

$$\boldsymbol{y}^s[n]\triangleq\boldsymbol{S}[n]\boldsymbol{y}[n] \tag{2}$$

and $\mathbf{y}[n]=\big[y_1[n],y_2[n],\ldots,y_K[n]\big]^{\mathsf{T}}\triangleq\boldsymbol{x}+\boldsymbol{v}[n]$, where $\boldsymbol{S}[n]$ denotes a random sampling matrix defined as

$$\boldsymbol{S}[n]=[\boldsymbol{e}_{k_{1n}},\boldsymbol{e}_{k_{2n}},\ldots,\boldsymbol{e}_{k_{Mn}}]^{\mathsf{T}}\in\{0,1\}^{M\times K} \tag{3}$$

and $\boldsymbol{e}_{k_{mn}}$ is a length-K unit vector in which the k_{mn}th entry is one and all other entries are zero. Besides, $\boldsymbol{v}[n]\triangleq\big[v_1[n],v_2[n],\ldots,v_K[n]\big]^{\mathsf{T}}$ is a zero-mean, spatially and temporally independent Gaussian noise with covariance $\boldsymbol{C}[n]\triangleq\mathrm{diag}\{\sigma_1^2,\sigma_2^2,\ldots,\sigma_K^2\}$.

2. Problem formulation

In this paper, we consider the problem of recovering the graph signal $\boldsymbol{x}$ from M low-resolution multi-bit quantized data $\boldsymbol{d}[n]$, not directly from the noisy samples $\mathbf{y}^s[n]$. Assume that each node $k\in\mathcal{V}$ is equipped with a random generator (RG) and a quantizer. At time n, each RG can provide a zero-mean random dithering $r_k[n]$ [20], [21] with variance 1. Using $r_k[n]$, the quantizer can produce a low-resolution multi-bit output $d_k[n]=Q(z_k[n])$, $k\in\mathcal{V}$, as shown in Figure 1, where

$$z_k[n]=r_k[n]y_k \ \text{ and } \ y_k[n]\triangleq x_k+v_k[n] \tag{4}$$

and Q denotes an element-wise mid-tread type uniform quantizer defined as

$$Q(z)=\omega_h \ \text{ if } \ \alpha_h\leq z<\alpha_{h+1} \tag{5}$$

and $\alpha_1<\alpha_2<\cdots<0<\cdots<\alpha_{2^q-2}<\alpha_{2^q-1}$ are the 2^q-1 threshold levels. The random dithering $r_k[n]$ makes the quantizer's input be zero-mean and helps to set the quantization thresholds. In this paper, the low-resolution multi-bit quantized data means that $q=1$–4. As q increases, the resolution gets higher and higher, and in particular $d_k[n]=z_k[n]$ for $q=+\infty$ (infinite-bit quantization or full-precision).

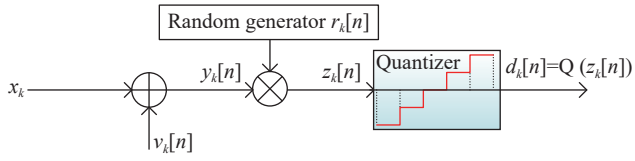

Figure 1 Low-resolution multi-bit quantized signal model.

III. Multi-Bit Graph Signal Recovery (MB-GSR)

In this section, we formulate a maximum likelihood problem whose solution provides us with an estimate of $\boldsymbol{x}$ by using the q-bit quantized observations

$$\mathcal{D}^s = \{\boldsymbol{d}^s[1], \boldsymbol{d}^s[2], \ldots, \boldsymbol{d}^s[T]\} \in \mathbb{R}^{M\times T} \tag{6}$$

are taken over a random node subsets $\{\mathcal{V}^s[n], n = 1, 2, \ldots, T\}$ with $T \geq 1$. Moreover,

$$\boldsymbol{d}^s[n] \triangleq \left[d_{k_{1n}}[n], d_{k_{2n}}[n], \ldots, d_{k_{Mn}}[n]\right]^{\mathsf{T}} = Q(\mathbf{z}^s[n]) \tag{7}$$

and $\boldsymbol{z}^s[n] \triangleq \left[z_{k_{1n}}[n], z_{k_{2n}}[n], \ldots, z_{k_{Mn}}[n]\right]^{\mathsf{T}}$ defined by

$$\boldsymbol{z}^s[n] \triangleq \boldsymbol{S}[n]\mathbf{z}[n] = \boldsymbol{S}[n]\boldsymbol{\Lambda}[n]\mathbf{x} + \boldsymbol{\vartheta}[n] \tag{8}$$

with

$$\boldsymbol{z}[n] \triangleq \left[z_1[n], z_2[n], \ldots, z_K[n]\right]^{\mathsf{T}} \tag{9}$$

$$\boldsymbol{\Lambda}[n] \triangleq \mathrm{diag}(r_1[n], r_2[n], \ldots, r_M[n]) \tag{10}$$

$$\boldsymbol{\vartheta}[n] \triangleq \boldsymbol{S}[n]\boldsymbol{\Lambda}[n]\mathrm{v}[n] \tag{11}$$

Moreover, $\boldsymbol{\vartheta}[n]$ is a zero-mean Gaussian random vector with covariance $\boldsymbol{C}^s[n] \triangleq \mathrm{diag}\{\sigma^2_{k_{1n}}, \sigma^2_{k_{2n}}, \ldots, \sigma^2_{k_{Mn}}\}$.

To be specific, we assume that the center processor can duplicate the same random variable $r_k[n]$. For example, each node k generates its $r_k[n]$ from a random sequence generator with different seeds, and these seeds are known to the center processor, so that the corresponding input vectors can be duplicated in the center processor [17], [22]. In this case, we consider to recover $\boldsymbol{x}$ via maximizing a regularized maximum-likelihood function:

$$\mathcal{L}(\boldsymbol{x}) = \log P(\mathcal{D}^s|\boldsymbol{x}) - \gamma\boldsymbol{x}^{\mathsf{T}}\boldsymbol{L}\boldsymbol{x} \tag{12}$$

where the second term $\boldsymbol{x}^{\mathsf{T}}\boldsymbol{L}\boldsymbol{x} = \frac{1}{2}\sum_{i\in\mathcal{V}}\sum_{j\in\mathcal{V}}(x_j - zx_i)^2 w_{ij}$ is the regularization that measures the smoothness, $\boldsymbol{L}$ is the Laplacian matrix, and γ is a factor balancing the trade-off between smoothness and data-fitting. For equation (12), it is hard to directly maximize $\log P(\mathcal{D}^s|\boldsymbol{x})$ with $\boldsymbol{x}$. Hence, we find an auxiliary lower bound of the log likelihood $\log P(\mathcal{D}^s|\boldsymbol{x})$:

$$\begin{aligned}
&\log P(\mathcal{D}^s|\boldsymbol{x}) \\
&= \int \log P(\mathcal{D}^s, \mathcal{Z}^s|\boldsymbol{x}) d\mathcal{Z}^s \\
&\geq \left\langle \left[\log \frac{P(\mathcal{D}^s, \mathcal{Z}^s|\boldsymbol{x})}{P(\mathcal{Z}^s|\mathcal{D}^s, \hat{\boldsymbol{x}})}\right] \right\rangle_{P(\mathcal{Z}^s|\mathcal{D}^s,\hat{\boldsymbol{x}})} \triangleq F(\boldsymbol{x}|\hat{\boldsymbol{x}})
\end{aligned} \tag{13}$$

In (13), $\mathcal{Z}^s = \{\boldsymbol{z}^s[1], \boldsymbol{z}^s[2], \ldots, \boldsymbol{z}^s[T]\} \in \mathbb{R}^{M\times T}$, and $\mathbb{E}_{P(\mathcal{Z}^s|\mathcal{D}^s,\hat{\boldsymbol{x}})}[\cdot]$ denotes the expectation over $P(\mathcal{Z}^s|\mathcal{D}^s, \hat{\boldsymbol{x}})$. Moreover, $\langle x\rangle_{P(x)}$ denotes an expectation over the distribution $P(x)$.

The lower bound $F(\boldsymbol{x}|\hat{\boldsymbol{x}})$ is a simple consequence of Jensen's inequality for the log function, and it paves the way for iteratively solving the problem $\max_{\boldsymbol{x}} \mathcal{L}(\boldsymbol{x})$. Since we have not access to the original noisy samples $\mathcal{Y}$, we treat them as latent variables and employ the expectation maximization (EM) scheme. Given an initialization $\hat{\boldsymbol{x}}_0$, the EM iteration performs coordinate ascent on the lower bound $F(\boldsymbol{x}|\hat{\boldsymbol{x}}_\ell) - \gamma\boldsymbol{x}^{\mathsf{T}}\boldsymbol{L}\boldsymbol{x}$, that is,

$$\begin{aligned}
&\hat{\boldsymbol{x}}_{\ell+1} \\
&= \arg\max_{\boldsymbol{x}} \left\{F(\boldsymbol{x}|\hat{\boldsymbol{x}}_\ell) - \gamma\boldsymbol{x}^{\mathsf{T}}\boldsymbol{L}\boldsymbol{x}\right\} \\
&= \arg\max_{\boldsymbol{x}} \left\{\left\langle \log P(\mathcal{Z}^s|\boldsymbol{x})\right\rangle_{P(\mathcal{Z}^s|\mathcal{D}^s,\hat{\boldsymbol{x}}_\ell)} - \gamma\boldsymbol{x}^{\mathsf{T}}\boldsymbol{L}\boldsymbol{x}\right\}
\end{aligned} \tag{14}$$

where $\ell = 0, 1, 2, \ldots$ denotes the EM-iteration index. In the second line of (14), we have removed some constants which do not depend on $\boldsymbol{x}$. From the graph signal sampling model (8), the conditional expectation in (14) can be expanded as

$$\begin{aligned}
&\left\langle \log P(\mathcal{Z}^s|\boldsymbol{x})\right\rangle_{P(\mathcal{Z}^s|\mathcal{D}^s,\hat{\boldsymbol{x}}_\ell)} \\
&= -\sum_{n=1}^{T} \left\langle \left|\, |\boldsymbol{z}^s[n] - \boldsymbol{S}[n]\boldsymbol{\Lambda}[n]\mathbf{x}|\, \right|^2_{\bar{\boldsymbol{C}}^s[n]} \right\rangle_{P(\boldsymbol{z}^s[n]|\boldsymbol{d}^s[n],\hat{\boldsymbol{x}}_\ell)} \\
&\quad + const \\
&= -\sum_{n=1}^{T} \left|\, \left|\boldsymbol{\eta}_\ell[n] - \boldsymbol{S}[n]\boldsymbol{\Lambda}[n]\mathbf{x}\right| \,\right|^2_{\bar{\boldsymbol{C}}^s[n]} + const
\end{aligned} \tag{15}$$

where *const*s denote constants with respect to $\boldsymbol{x}$, $\|\boldsymbol{x}\|^2_{\boldsymbol{C}} = \boldsymbol{x}^{\mathsf{T}}\boldsymbol{C}\boldsymbol{x}$, $\bar{\boldsymbol{C}} \triangleq \boldsymbol{C}^{-1}$, and

$$\boldsymbol{\eta}_\ell[n] \triangleq \langle \boldsymbol{z}^s[n]\rangle_{P(\mathbf{y}^s[n]|\boldsymbol{d}^s[n],\hat{\boldsymbol{x}}_\ell)} = \left[\eta_{\ell,1}[n], \eta_{\ell,2}[n], \ldots, \eta_{\ell,M}[n]\right]^{\mathsf{T}}$$

Plugging (15) into (14) and ignoring the constants, it follows that

$$\begin{aligned}
&\hat{\boldsymbol{x}}_{\ell+1} \\
&= \arg\min_{\boldsymbol{x}} \left\{\frac{1}{T}\sum_{n=1}^{T} \left\|\boldsymbol{\eta}_\ell[n] - \boldsymbol{S}[n]\boldsymbol{\Lambda}[n]\boldsymbol{x}\right\|^2_{\bar{\boldsymbol{C}}^s[n]} + \gamma\boldsymbol{x}^{\mathsf{T}}\boldsymbol{L}\boldsymbol{x}\right\}.
\end{aligned}$$

This requires $(\boldsymbol{G} + \gamma\boldsymbol{L})\,\hat{\boldsymbol{x}}_{\ell+1} = \boldsymbol{h}_\ell$ where

$$\boldsymbol{G} \triangleq \frac{1}{T}\sum_{n=1}^{T}\sum_{m=1}^{M} \sigma^{-2}_{k_{mn}} r^2_{k_{mn}}[n]\boldsymbol{e}_{k_{mn}}\boldsymbol{e}^{\mathsf{T}}_{k_{mn}} \tag{16}$$

$$\boldsymbol{h}_\ell \triangleq \frac{1}{T}\sum_{n=1}^{T}\sum_{m=1}^{M} \sigma^{-2}_{k_{mn}} \eta_{\ell,m}[n] r_{k_{mn}}[n]\boldsymbol{e}_{k_{mn}} \tag{17}$$

It is readily deduced that the following lemma is true, see Appendix A.

Lemma 1 Matrix $\boldsymbol{G} + \gamma\boldsymbol{L}$ is always invertible for $\gamma \neq 0$ and any sampled subset of the graph nodes.

Using Lemma 1, we obtain the solution as $\hat{\boldsymbol{x}}_{\ell+1} = (\boldsymbol{G} + \gamma\boldsymbol{L})^{-1}\boldsymbol{h}_\ell$. However, our work is not finished, the estimate $\hat{\boldsymbol{x}}_{\ell+1}$ depends on $\boldsymbol{\eta}_\ell[n]$ and we have yet to compute it. Since each element $d^s_m[n] \triangleq d_{k_{mn}}[n]$ of the observation vector $\boldsymbol{d}^s[n]$ determines a lower bound $\tau^-_m[n]$ and

an upper bound $\tau_m^+[n]$ for $z_m^s[n] \triangleq z_{k_{mn}}[n]$, $\forall\ m \in \mathcal{M} \triangleq \{1,2,\ldots,M\}$ and $n \in \mathcal{T} \triangleq \{1,2,\ldots,T\}$, it holds that

$$P(\boldsymbol{z}^s[n]|\boldsymbol{d}[n],\hat{\boldsymbol{x}}_\ell) = \prod_{m=1}^{M}\prod_{n=1}^{T} P(z_m^s[n]|\tau_m^-[n] \le z_m^s[n] \le \tau_m^+[n],\hat{\boldsymbol{x}}_\ell) \tag{18}$$

In addition, we recall the following lemma [22].

Lemma 2 Given a random v with standard normal distribution, and two constants a and b satisfying $a > b$, it holds that for the conditional first-order moments of v: $\mathbb{E}[v|b < v < a] = \frac{\varphi(b)-\varphi(a)}{\Phi(a)-\Phi(b)}$, where $\varphi(\cdot)$ and $\Phi(\cdot)$ respectively denote the probability density function and the cumulative distribution function of the standard normal distribution.

By this lemma and equation (18), it follows that

$$\begin{aligned}\eta_{\ell,m}[n] &= \langle z_m^s[n]\rangle_{P(z_m^s[n]|\tau_m^-[n]\le z_m^s[n]\le\tau_m^+[n],\hat{\boldsymbol{x}}_\ell)} \\ &= r_{k_{mn}}\hat{x}_{k_{mn},\ell} + \sigma_{k_{mn}}\frac{\varphi(\varsigma_m^-[n]) - \varphi(\varsigma_m^+[n])}{\Phi(\varsigma_m^+[n]) - \Phi(\varsigma_m^-[n])}\end{aligned} \tag{19}$$

for $m = 1,2,\ldots,M$, with

$$\varsigma_m^+[n] \triangleq \frac{\tau_m^+[n] - r_{k_{mn}}\hat{x}_{k_{mn},\ell}}{\sigma_{k_{mn}}}$$
$$\varsigma_m^-[n] \triangleq \frac{\tau_m^-[n] - r_{k_{mn}}\hat{x}_{k_{mn},\ell}}{\sigma_{k_{mn}}}$$

In this way, the MB-GSR algorithm can be summarized as Algorithm 1.

Algorithm 1 MB-GSR Algorithm

Input: K, M, $\boldsymbol{L}$, γ, $\{\alpha_1,\alpha_2,\ldots,\alpha_{2q-1}\}$, $\{r_k[n], k\in\mathcal{K}\}$, $\mathcal{V}^s[n] = \{k_{mn}, m \in \mathcal{M}\}$, $\boldsymbol{d}^s[n]$, for all $n \in \mathcal{T}$, $\{\alpha_1,\alpha_2,\ldots,0,\ldots,\alpha_{2q},\alpha_{2q-1}\}$.

1: **Initialize** $\{\hat{x}_m, m\in\mathcal{V}\}$;

2: $\boldsymbol{G} = \frac{1}{T}\sum_{n=1}^{T}\sum_{m=1}^{M}\sigma_{k_{mn}}^{-2} r_{k_{mn}}^2[n]\boldsymbol{e}_{k_{mn}}\boldsymbol{e}_{k_{mn}}^{\mathsf{T}}$;

3: $\boldsymbol{P} = (\boldsymbol{G}+\gamma\boldsymbol{L})^{-1}$;

4: **Repeat** ($n \in \mathcal{T}$, $m \in \mathcal{M}$, $k_{mn} \in \mathcal{V}^s[n]$)

5: $\varsigma_m^+[n] = \frac{\tau_m^+[n]-r_{k_{mn}}\hat{x}_{k_{mn}}}{\sigma_{k_{mn}}}$;

6: $\varsigma_m^-[n] = \frac{\tau_m^-[n]-r_{k_{mn}}\hat{x}_{k_{mn}}}{\sigma_{k_{mn}}}$;

7: $\Omega_m[n] = \frac{\varphi(\varsigma_m^-[n])-\varphi(\varsigma_m^+[n])}{\Phi(\varsigma_m^+[n])-\Phi(\varsigma_m^-[n])}$;

8: $\eta_m[n] = r_{k_{mn}}\hat{x}_{k_{mn}} + \sigma_{k_{mn}}\Omega_m[n]$;

9: $\boldsymbol{h} = \frac{1}{T}\sum_{n=1}^{T}\sum_{m=1}^{M}\sigma_{k_{mn}}^{-2}\eta_m[n]r_{k_{mn}}[n]\boldsymbol{e}_{k_{mn}}$;

10: $\hat{\boldsymbol{x}} = \boldsymbol{P}\boldsymbol{h}$;

11: **Until** stopping criterion is satisfied

Output: $\hat{\boldsymbol{x}} = [\hat{x}_1,\hat{x}_2,\ldots,\hat{x}_K]^{\mathsf{T}}$.

A major computational complexity here lies in the inversion of the matrix $\boldsymbol{G}+\gamma\boldsymbol{L}$, which usually is order K^3 and increases with the size K of the graph. Fortunately, the matrix inversion can be performed in advance before the algorithm starts to run. Another major computational complexity of the proposed algorithm comes from the EM iterations. This involves about $(TM+K^2)N$ multiplications where N is the number of the EM iterations.

In addition, although this paper considers undirected graphs, the proposed MB-GSR algorithm with a small modification can also be applied to the case of directed graphs. For directed graphs, it holds that

$$\sum_{i\in\mathcal{V}}\sum_{j\in\mathcal{V}}(x_j - x_i)^2 w_{ij} = \boldsymbol{x}^{\mathsf{T}}(\tilde{\boldsymbol{L}}+\boldsymbol{L})\boldsymbol{x}$$

with $\tilde{\boldsymbol{L}}=\tilde{\boldsymbol{D}}-\boldsymbol{W}^{\mathsf{T}}$, $\tilde{\boldsymbol{D}}=\mathrm{diag}(\sum_{i\in\mathcal{V}}w_{i1},\sum_{i\in\mathcal{V}}w_{i2},\ldots,\sum_{i\in\mathcal{V}}w_{iK})$. Therefore, in this case, the solution to problem (14) is given by

$$\hat{\boldsymbol{x}}_{\ell+1} = \left(\boldsymbol{G}+\frac{1}{4}\gamma(\tilde{\boldsymbol{L}}+\boldsymbol{L}+\tilde{\boldsymbol{L}}^{\mathsf{T}}+\boldsymbol{L}^{\mathsf{T}})\right)^{-1}\boldsymbol{x}_\ell$$

IV. Simulation Results

In this section, numerical results are provided for assessing the performance of the proposed MB-GSR algorithm for recovering a smooth graph signal $\boldsymbol{x}^0$ from low-resolution few-bit the q-bit quantized observations ($q = 1,2,3,4$). For the case of $q=\infty$ (i.e., graph signal recovery from unquantized observations), the corresponding algorithm is similar to some existing algorithms based on smoothness penalties [2], [10], [23]. The recovery performance is quantified in terms of the normalized mean squared reconstruction error $\mathrm{MSE} = \mathbb{E}|\,|\hat{\boldsymbol{x}}-\boldsymbol{x}_0|\,|^2/K$, and the signal-to-noise ratio (SNR) is defined as $\mathrm{SNR} \triangleq -20\times\log\sum_{k=1}^{K}\sigma_k$. All results described below have been obtained by averaging over 100 independent realizations of the sampling set and the noise. Moreover, without loss of generality, we use the GraSP toolbox [24] to yield a signal $\boldsymbol{x}_0$ over a graph with $K = 200$ nodes, as shown in Figure 2.

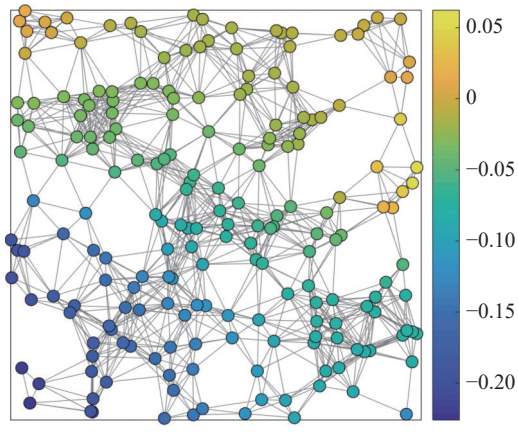

Figure 2 Signal $\boldsymbol{x}_0$ over a graph with $K = 200$ nodes.

Figure 3 presents scattering diagrams of the graph signal recovery using the proposed MB-GSR algorithm. Here, the factor $\gamma = 0.9$, SNR = 20 dB, and $T = 800$ quantized/unquantized observations are used. Moreover,

three cases of the sampling ratio $M/K = 10\%$, 30%, and 50%, respectively, are considered, that is, $M = 20$, 60, and 100 nodes out of a total 200 nodes respectively are sampled, as shown in Figure 3(a), (d), and (g). The recovery results using the 2-bit GSR algorithm are shown in Figure 3(b), (e), and (h), respectively, and those using the ∞-bit GSR algorithm [10] from the unquantized observations are shown in Figure 3(c), (f), and (i), respectively.

From Figure 3, we can observe that, as the sampling ratio M/K increases, the recovery graph signals obtained by using both the 2-bit GSR algorithm and the ∞-bit GSR algorithm become more and more similar to the true graph signal. This shows that the performance of the 2-bit GSR algorithm is comparable to that of the ∞-bit GSR algorithm.

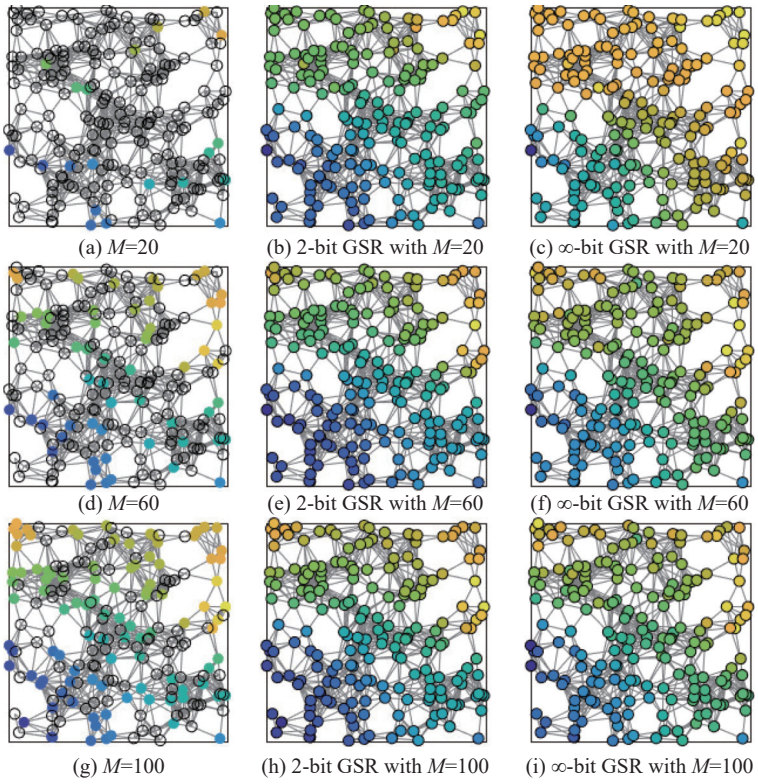

Figure 3 Scattering diagrams of the graph signal recovery wth the sampling ratio $M/K = 10\%$ (M=20), 30% (M=60), and 50% (M=100), respectively, where the unfilled circles in (a), (d), and (g) denote the unsampled nodes.

We now consider a real-world dataset of the sea surface temperature (SST) [25], which is published by the Physical Sciences Laboratory. It is collected weekly from October 1881 to December 1989, and the spatial resolution is 1° latitude × 1° longitude. We randomly select SSTs of $K = 2000$ points from 0° west longitude to 360° west longitude, and 90° south latitude to 90° north latitude. As shown in Figure 4, the SSTs of theses 2000 points are constructed as a graph $\mathcal{G} = (\mathcal{V}, \mathcal{E}, \boldsymbol{W})$ by using a 4-nearest neighbors algorithm with the weight of each edge inversely proportional to the square of the distance between its two nodes. We can recover the SSTs from their M low-resolution multi-bit quantized data to further evaluate the performance of the MB-GSR algorithm.

Figure 5 depicts the MSEs versus the sampling ratio in the range $M/K = 10\%, \ldots, 90\%$ with $T = 800$ quantized/unquantized observations and SNR = 20 dB. It is seen that the recovery performance of all schemes improves with increasing sampling ratio, and moreover, increasing the number of quantization bits from 1-bit to 2-bit and then to 4-bit leads to a considerable performance improvement. Further, it is observed that the MSE of 4-bit GSR is very close to that of the ∞-bit GSR from the unquantized observations.

Figure 6 plots the MSEs versus the SNR varying from -5 dB to 15 dB with $M/K = 0.4$ and the number

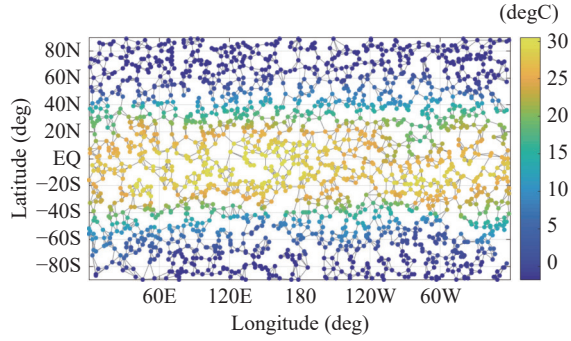

Figure 4 Sea surface temperature dataset over a graph with $K = 2000$ points.

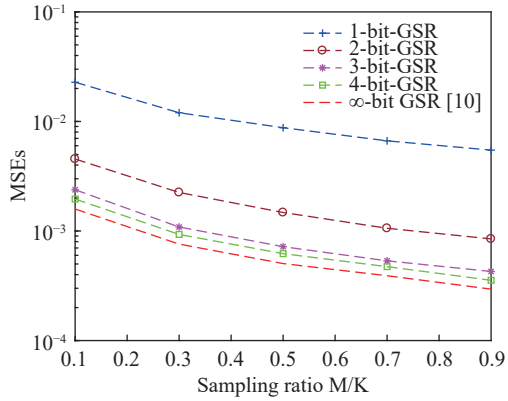

Figure 5 MSEs of the MB-GSR algorithm versus the sampling ratio M/K.

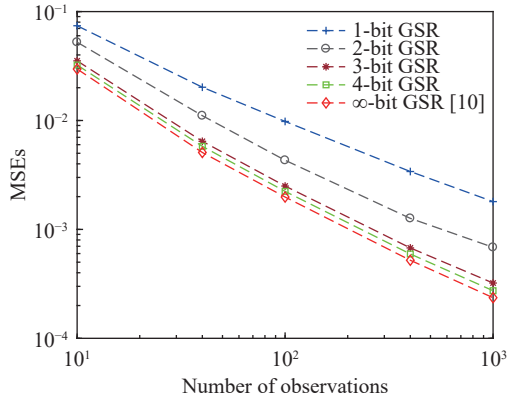

Figure 7 MSEs of the MB-GSR algorithm versus the number of observations.

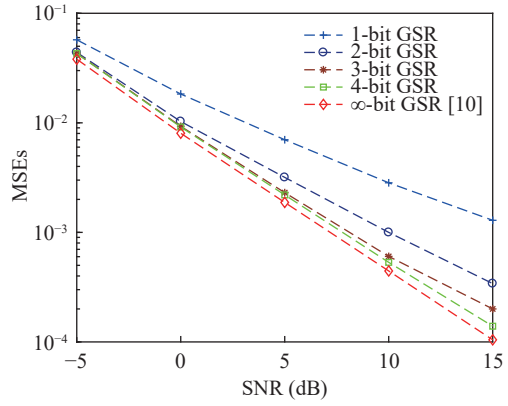

Figure 6 MSEs of the MB-GSR algorithm versus the SNR.

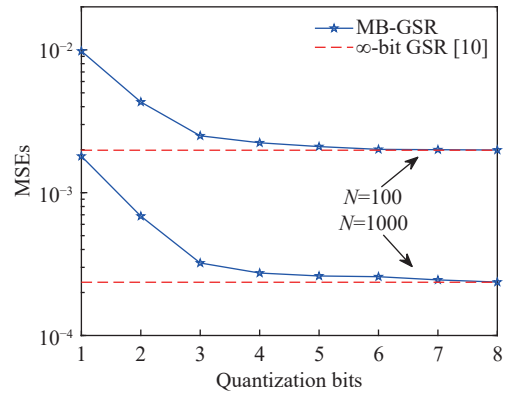

Figure 8 MSEs of the GSR algorithm (∞-bit quantization) [10] and the proposed MB-GSR algorithm versus the number of quantization bits.

of quantized/unquantized observations $T = 600$. We find that the proposed MB-GSR algorithm using 3-bit or 4-bit quantized observations has almost similar recovery accuracy to that of the ∞-bit GSR using the unquantized observations.

Figure 7 plots the MSEs versus the number of observations T varying from 10 to 10000 with $M/K = 0.4$ and SNR=20 dB. This figure shows that, to achieve an MSE of 2×10^{-3} for example, ∞-bit, 4-bit, 3-bit, 2-bit and 1-bit cases need about 100, 120, 150, 300 and 1000 observations, respectively. This indicates that the total number of bits required to achieve an MSE of 2×10^{-3} is, respectively, 480, 450, 600, and 1000 bits for 4-bit, 3-bit, 2-bit, and 1-bit quantization scenarios.

Figure 8 further presents the comparison result of the ∞-bit GSR algorithm and the proposed MB-GSR algorithm versus the number of quantization bits with $M/K = 0.4$, SNR=20 dB, $T = 100$ and 1000. The figure shows that the proposed MB-GSR algorithm with 4-bit quantized observations has achieved reconstruction accuracy similar to the ∞-bit GSR algorithm.

Note that the ∞-bit GSR requires high-resolution ADCs, whose implementation costs and power consumption are much higher compared to 3-bit and 4-bit ADCs. For instance, a 14-bit ADC with sampling frequency of 10 MHz consumes almost 10^3 times more power than 3-bit and 4-bit ADCs with the same sampling frequency [16].

V. Conclusions

In this paper, we investigated the problem of reconstructing smooth graph signals from low-resolution multi-bit sampling observations taken on a small number of graph nodes. The low-resolution multi-bit grasp signal sampling model was established by using an random dither quantizer, and the multi-bit graph signal recovery algorithms were developed. The simulation results revealed that the grasp recovery performance could be substantially improved when increasing the sampling resolution from 1-bit quantization case to 2 or 4 bits per sampling observations, while the power consumption and implementation costs remain much lower than the high-resolution sampling scenario.

There are several possible extensions to this work that may be interesting lines of future research. To further improve performance, the non-uniform quantization (e.g., Lloyd-Max quantization) may be used to replace the uniform quantization in this paper. Graph topology identification is required for the case where the adjacency matrix or edge weight matrix is unknown. Hence, how to implement the identification task by using the low-bit observations is still open questions that are worth fur-

ther studying.

Acknowledgement

This work was supported by the National Natural Science Foundation of China (Grant No. 61671192) and the Opening Foundation of Zhejiang Engineering Research Center of MEMS (Grant No. MEMSZJERC2204).

Appendix A. The Derivation of Lemma 1

By definitions $\boldsymbol{G}$ is a diagonal matrix with the non-negative diagonal elements $\{[\boldsymbol{G}]_{kk} \geq 0, k = 1, 2, \ldots, K\}$. There exist two cases:

1) All diagonal elements are positive: $[\boldsymbol{G}]_{kk} > 0$ for $k = 1, 2, \ldots, K$, which corresponds to the case that each node of the graph is sampled at least once during $n = 1, 2, \ldots, T$. In this case, $\boldsymbol{G}$ is full rank and hence the matrix sum $\boldsymbol{H} \triangleq \boldsymbol{G} + \gamma \boldsymbol{L}$ is also full rank since $\det(\boldsymbol{H}) \geq \det(\boldsymbol{G}) + \det(\gamma \boldsymbol{L}) = \det(\boldsymbol{G}) > 0$.

2) At least one diagonal element is 0: $\exists\ k \in \mathcal{V}$, $[\boldsymbol{G}]_{kk} = 0$, which corresponds to the case that there is at least one node that has never been sampled during $n = 1, 2, \ldots, T$. In this case, $0 < \mathrm{Rank}(\boldsymbol{G}) \leq K - 1$. Now, let $\boldsymbol{L}[r]$ be a submatrix of $\boldsymbol{L}$ which is obtained by deleting the rth row and the rth column of $\boldsymbol{L}$. By properties of the Laplacian matrix, $\boldsymbol{L}[r]$ is full rank for any r, and the rank of $\boldsymbol{L}$ is equal to $K - 1$, i.e., $\mathrm{Rank}(\boldsymbol{L}) = \mathrm{Rank}(\boldsymbol{L}[r]) = K - 1$, for any $r = 1, 2, \ldots, K$. Therefore, $\det(\boldsymbol{H}[r]) \geq \det(\boldsymbol{G}[r]) + \det(\gamma \boldsymbol{L}[r]) > 0$, that is, matrix $\boldsymbol{H}[r]$ is full rank for any r.

Without loss of generality, assume that node K has never been sampled, then $[\boldsymbol{G}]_{KK} = 0$ and $[\boldsymbol{H}]_{KK} = \gamma[\boldsymbol{L}]_{KK}$. We write $\boldsymbol{H}$ and $\boldsymbol{L}$ in the form of block matrices:

$$\boldsymbol{H} = \begin{bmatrix} \boldsymbol{H}[K] & -\gamma \boldsymbol{w}_K \\ -\gamma \boldsymbol{w}_K^{\mathsf{T}} & \gamma[\boldsymbol{L}]_{KK} \end{bmatrix} \text{ and } \boldsymbol{L} = \begin{bmatrix} \boldsymbol{L}[K] & -\boldsymbol{w}_K \\ -\boldsymbol{w}_K^{\mathsf{T}} & [\boldsymbol{L}]_{KK} \end{bmatrix}$$

where $\boldsymbol{w}_K = [w_{1K}, w_{2K}, \ldots, w_{K-1,K}]^{\mathsf{T}}$ and $[\boldsymbol{L}]_{KK} = \boldsymbol{w}_K^{\mathsf{T}} \boldsymbol{1}_{K-1}$. It follows that

$$\det(\boldsymbol{L}) = \left([\boldsymbol{L}]_{KK} - w_K^{\top} (\boldsymbol{L}[K])^{-1} w_K \right) \cdot \det(L[K])$$

Because of $\det(\boldsymbol{L}) = 0$ and $\det(\boldsymbol{L}[K]) \neq 0$, we have

$$[\boldsymbol{L}]_{KK} = \boldsymbol{w}_K^{\mathsf{T}} (\boldsymbol{L}[K])^{-1} \boldsymbol{w}_K \tag{A-1}$$

Using this, we further get

$$\begin{aligned} \det(\boldsymbol{H}) &= \gamma \left([\boldsymbol{L}]_{KK} - \gamma \boldsymbol{w}_K^{\mathsf{T}} (\boldsymbol{H}[K])^{-1} \boldsymbol{w}_K \right) \cdot \det(\boldsymbol{H}[K]) \\ &= \gamma \boldsymbol{w}_K^{\mathsf{T}} \left((\boldsymbol{L}[K])^{-1} - \gamma (\boldsymbol{H}[K])^{-1} \right) \boldsymbol{w}_K \cdot \det(\boldsymbol{H}[K]) \end{aligned}$$

Since $\det(\boldsymbol{H}[K]) > 0$ and $\boldsymbol{H}[K] \neq \gamma \boldsymbol{L}[K]$, we deduce that $\det(\boldsymbol{H}) \neq 0$.

Again, we consider an extreme case where only one element is nonzero, for example : $[\boldsymbol{G}]_{KK} \neq 0$ and $[\boldsymbol{G}]_{kk} = 0$, $k = 1, 2, \ldots, K - 1$. We write $\boldsymbol{H}$ as

$$\boldsymbol{H} = \begin{bmatrix} \gamma \boldsymbol{L}[K] & -\gamma \boldsymbol{w}_K \\ -\gamma \boldsymbol{w}_K^{\mathsf{T}} & [\boldsymbol{H}]_{KK} \end{bmatrix}$$

Using the relation (A-1) again, we have

$$\begin{aligned} \det(\boldsymbol{H}) &= \gamma \left([\boldsymbol{H}]_{KK} - \gamma \boldsymbol{w}_K^{\top} (\boldsymbol{L}[K])^{-1} \boldsymbol{w}_K \right) \cdot \det(\boldsymbol{L}[K]) \\ &= \gamma \left([\boldsymbol{H}]_{KK} - \gamma [\boldsymbol{L}]_{KK} \right) \cdot \det(\boldsymbol{L}[K]). \end{aligned}$$

Since $\det(\boldsymbol{L}[K]) > 0$ and $[\boldsymbol{H}]_{KK} \neq \gamma [\boldsymbol{L}]_{KK}$, we also deduce that $\det(\boldsymbol{H}) \neq 0$. That is to say, matrix $\boldsymbol{H}$ is regular and reversible.

References

[1] A. Ortega, P. Frossard, J. Kovačević, *et al.*, "Graph signal processing: Overview, challenges, and applications," *Proceedings of the IEEE*, vol. 106, no. 5, pp. 808–828, 2018.

[2] D. I. Shuman, S. K. Narang, P. Frossard, *et al.*, "The emerging field of signal processing on graphs: Extending high-dimensional data analysis to networks and other irregular domains," *IEEE Signal Processing Magazine*, vol. 30, no. 3, pp. 83–98, 2013.

[3] L. H. Yang, Q. Zhang, Q. Zhang, *et al.*, "Atomic filter: A weak form of shift operator for graph signals," *Digital Signal Processing*, vol. 129, article no. 103644, 2022.

[4] T. T. Wang, H. Y. Guo, B. Lyu, *et al.*, "Speech signal processing on graphs: Graph topology, graph frequency analysis and denoising," *Chinese Journal of Electronics*, vol. 29, no. 5, pp. 926–936, 2020.

[5] E. Brugnoli, E. Toscano, and C. Vetro, "Iterative reconstruction of signals on graph," *IEEE Signal Processing Letters*, vol. 27, pp. 76–80, 2020.

[6] X. H. Wang, P. F. Liu, and Y. T. Gu, "Local-set-based graph signal reconstruction," *IEEE Transactions on Signal Processing*, vol. 63, no. 9, pp. 2432–2444, 2015.

[7] R. Torkamani, H. Zayyani, and F. Marvasti, "Joint topology learning and graph signal recovery using variational Bayes in non-Gaussian noise," *IEEE Transactions on Circuits and Systems II: Express Briefs*, vol. 69, no. 3, pp. 1887–1891, 2022.

[8] A. Anis, A. Gadde, and A. Ortega, "Efficient sampling set selection for bandlimited graph signals using graph spectral proxies," *IEEE Transactions on Signal Processing*, vol. 64, no. 14, pp. 3775–3789, 2016.

[9] X. W. Dong, D. Thanou, P. Frossard, *et al.*, "Learning Laplacian matrix in smooth graph signal representations," *IEEE Transactions on Signal Processing*, vol. 64, no. 23, pp. 6160–6173, 2016.

[10] K. Qiu, X. H. Mao, X. Y. Shen, *et al.*, "Time-varying graph signal reconstruction," *IEEE Journal of Selected Topics in Signal Processing*, vol. 11, no. 6, pp. 870–883, 2017.

[11] J. Z. Jiang, D. B. Tay, Q. Y. Sun, *et al.*, "Recovery of time-varying graph signals via distributed algorithms on regularized problems," *IEEE Transactions on Signal and Information Processing over Networks*, vol. 6, pp. 540–555, 2020.

[12] P. Di Lorenzo, P. Banelli, S. Barbarossa, *et al.*, "Distributed adaptive learning of graph signals," *IEEE Transactions on Signal Processing*, vol. 65, no. 16, pp. 4193–4208, 2017.

[13] S. H. Chen, R. Varma, A. Sandryhaila, *et al.*, "Discrete signal processing on graphs: Sampling theory," *IEEE Transactions on Signal Processing*, vol. 63, no. 24, pp. 6510–6523, 2015.

[14] P. Di Lorenzo, P. Banelli, E. Isufi, *et al.*, "Adaptive graph signal processing: Algorithms and optimal sampling strategies," *IEEE Transactions on Signal Processing*, vol. 66, no. 13, pp. 3584–3598, 2018.

[15] F. Wang, G. Cheung, and Y. C. Wang, "Low-complexity graph sampling with noise and signal reconstruction via neumann series," *IEEE Transactions on Signal Processing*, vol. 67, no. 21, pp. 5511–5526, 2019.

[16] R. H. Walden, "Analog-to-digital converter survey and analysis," *IEEE Journal on Selected Areas in Communications*, vol. 17, no. 4, pp. 539–550, 1999.

[17] Y. J. Chi and H. Y. Fu, "Subspace learning from bits," *IEEE Transactions on Signal Processing*, vol. 65, no. 17, pp. 4429–4442, 2017.

[18] S. Sedighi, M. R. B. Shankar, M. Soltanalian, *et al.*, "DOA estimation using low-resolution multi-bit sparse array measurements," *IEEE Signal Processing Letters*, vol. 28, pp. 1400–1404, 2021.

[19] J. Y. Hou, J. J. Wang, F. Zhang, *et al.*, "Robust reconstruction of block sparse signals from adaptively one-bit measurements," *Chinese Journal of Electronics*, vol. 29, no. 5, pp. 937–944, 2020.

[20] T. C. Aysal, M. J. Coates, and M. G. Rabbat, "Distributed

average consensus with dithered quantization," *IEEE Transactions on Signal Processing*, vol. 56, no. 10, pp. 4905–4918, 2008.

[21] D. K. W. Ho and B. D. Rao, "Antithetic dithered 1-bit massive MIMO architecture: Efficient channel estimation via parameter expansion and PML," *IEEE Transactions on Signal Processing*, vol. 67, no. 9, pp. 2291–2303, 2019.

[22] Z. T. Liu, C. G. Li, W. H. Zhuang, *et al.*, "Sparse robust learning from flipped bits," *IEEE Transactions on Signal Processing*, vol. 68, pp. 4407–4421, 2020.

[23] N. Thanou, "*Graph Signal Processing: Sparse Representation and Applications*," *Ph. D. Thesis*, vol. EPFL, article no. Lausanne,Swi, 2016.

[24] B. Girault, S. S. Narayanan, A. Ortega, *et al.* "Grasp: A matlab toolbox for graph signal processing," in *Proceedings of the 2017 IEEE International Conference on Acoustics, Speech and Signal Processing (ICASSP)*, New Orleans, LA, USA, pp. 6574–6575, 2017.

[25] "Sea surface temperature (SST) V2, 2015," Available at: https://psl.noaa.gov/data/gridded/data.noaa.oisst.v2.html, 2022.

Zhaoting LIU was born in 1975. He received the Ph.D. degree in electrical engineering at Nanjing University of Science and Technology, NanJing, China, in 2011. He is now with the School of Communication Engineering, Hangzhou Dianzi University, Hangzhou, China. His current research interests include radar signal processing, wireless sensor network, and adaptive filtering. (Email: liuzht@hdu.edu.cn)

Chen YU was born in 1998. She is an M.S. candidate at the School of Communication Engineering, Hangzhou Dianzi University, China. Her research direction is graph signal processing. (Email: yuchen102955@163.com)

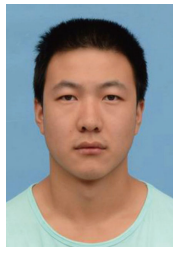

Yafeng WANG was born in 1996. He is an M.S. candidate at the School of Communication Engineering, Hangzhou Dianzi University, Hangzhou, China. His research interests include adaptive filtering and wireless sensor network. (Email: ab203230@126.com)

Shuchen LIU was born in 1999. She is an M.E. candidate at the School of Communication Engineering, Hangzhou Dianzi University, China. His research interests include wireless sensor network, target targeting and tracking. (Email: liushuchen1804@163.com)